Reproducibility and Reliability of Pancreatic Pharmacokinetic Parameters Derived from Dynamic Contrast-Enhanced Magnetic Resonance Imaging

Weiwei Zhao
Xi'an Hospital of Traditional Chinese Medicine
Jing Yu
The Fourth Military Medical University
Yuyu Bi
Xi'an Hospital of Traditional Chinese Medicine
Yi Huan
The Fourth Military Medical University
Yuanqiang Zhu
The Fourth Military Medical University
Weiqi Zhang
The Fourth Military Medical University
Jianmin Zheng
The Fourth Military Medical University
Zhiyong Quan (qzy1503@163.com)
The Fourth Military Medical University
Yong Yang
Xi'an Hospital of Traditional Chinese Medicine

Research Article

Keywords: Dynamic contrast-enhanced magnetic resonance imaging, Pancreas, Pharmacokinetic parameters, Reproducibility, Reliability

Posted Date: December 8th, 2021

DOI: https://doi.org/10.21203/rs.3.rs-1101008/v1

Abstract

Objectives

Dynamic contrast-enhanced MRI (DCE-MRI) with Extended Tofts Linear (ETL) model has been used in tissue and tumor evaluation. However, its reliability and reproducibility in pancreatic evaluation has been unclear. It is also unclear whether pancreatic DCE-MRI pharmacokinetic parameters were consistent and stable among different pancreatic regions, ages and genders.

Methods

Pancreatic pharmacokinetic parameters of 54 volunteers were calculated using DCE-MRI with ETL model. Firstly, Intra- and inter-observer reproducibility was evaluated using intra-class correlation coefficient (ICC) and coefficient of variation (CoV). Secondly, subgroup evaluation of pancreatic DCE-MRI pharmacokinetic parameters was performed. 54 subjects were divided into three groups in virtue of pancreatic region, three groups according to age, two groups according to gender, which pharmacokinetic parameters among and between different groups were calculated and compared.

Results

There was excellent agreement and low variability of intra- and inter-observer to pancreatic DCE-MRI pharmacokinetic parameters. The intra- and inter-observer ICCs of K^{trans}, k_{ep}, v_e, v_p were 0.971, 0.952, 0.959, 0.944 and 0.947, 0.911, 0.978, 0.917, respectively. The intra- and inter-observer CoVs of K^{trans}, k_{ep}, v_e, v_p were 9.98%, 5.99%, 6.47%, 4.76% and 10.15%, 5.22%, 6.28%, 5.40%, respectively. There were no significant differences of K^{trans}, k_{ep} among different pancreatic regions, among different age groups, between male and female groups (P all > 0.10). Only, pancreatic v_e of old group was higher than that of young and middle-aged groups (P = 0.042, 0.001), and v_p of pancreatic head was higher than that of pancreatic body and tail (P = 0.014, 0.043).

Conclusions

DCE-MRI with ETL model is reliable and reproducible for quantitative assessment of pancreatic pharmacokinetic parameters. v_e varies with age and v_p varies with pancreatic region, which can provide guidance for the selection of normal reference in the pharmacokinetics study of pancreatic diseases.

Introduction

The concept of dynamic MRI after contrast-agent injection was proposed in the mid-1980s, as a way of measuring the contribution of tissue perfusion and capillary permeability to the signal changes caused by the agent[1, 2]. Dynamic MRI can be used to non-invasively assess normal or diseased tissue perfusion and micro-vessel permeability by means of qualitative, semi-quantitative and quantitative methods[3–5]. With the inclusion of arterial input function(AIF)and pharmacokinetic models, quantitative dynamic contrast-enhanced MRI (DCE-MRI) has been demonstrated superior to either qualitative or semi-quantitative method with respect to accurate acquisition of pharmacokinetic parameters[6]. However, the differences of AIF and pharmacokinetic models will affect the reliability and reproducibility of DCE-MRI pharmacokinetic parameters[7–9]. Among the practicable pharmacokinetic models, Extended Tofts Linear (ETL) model as a representative of two-compartment model can be recommended for quantitative assessment of physiological and pathological features, and a series of reliable results have been obtained[9, 10]. The pancreas is an important digestive organ, which can undergo a variety of neoplastic and non-neoplastic lesions[11, 12]. Accurate evaluation of the pancreas using DCE-MRI is helpful in diagnosis and differential diagnosis. However, pancreas is susceptible to respiratory motion and gastrointestinal peristalsis, whether the pancreatic pharmacokinetic parameters deriving from DCE-MRI with ETL model are robust, which needs to be further explored.

Pancreas is divided into pancreatic head, body and tail, and there is a different source of the blood supply for each region[13]. Besides, pancreatic parenchyma ratio varies for different age groups due to pancreatic atrophy and fat replacement[14], and some pancreatic tumors have certain gender tendency. In DCE-MRI assessment of pancreatic lesion, adjacent non-lesion pancreatic parenchyma on the same patient or pancreas from other healthy control are generally selected as normal reference[15, 16]. However, those previous studies always ignored the influence of different pancreatic regions, age and gender on pancreatic pharmacokinetic parameters. Hence, whether

the DCE-MRI pharmacokinetic parameters of the pancreas are consistent across different pancreatic regions, age and gender distributions, which is worth exploring and needing to be clarified before the study of pancreatic disease and selection of control group.

Thus, in the present study, we evaluated the reliability and reproducibility of pancreatic pharmacokinetic parameters derived from DCE-MRI with ETL model, and provided the relationship between pancreatic DCE-MRI parameters and 3 factors (pancreatic region, gender, and age) on the purpose of providing a reference for future study of pancreatic disease and selection of normal control.

Methods

This study was in accordance with the 1964 Helsinki Declaration and its later amendments or comparable ethical standards. The study was approved by the ethics committee of the Xijing Hospital of Air Force Military Medical University. The informed consent was obtained from all participants before collecting information. Data were analyzed and interpreted by the authors. All the authors reviewed the manuscript and vouch for the accuracy and completeness of the data and for the adherence of the study to the protocol.

Subjects

66 volunteers were recruited to participate the study from May 2019 to February 2020. To be included in this study, subjects had to meet the following inclusion criteria: more than 18 years old, healthy and with normal pancreatic function, no any disease influencing pancreas. Exclusion criteria included common exclusion criteria for MRI scans and the use of Gd-related contrast agent, subjects with atherosclerotic disease influencing AIF, and poor DCE-MRI image quality. Poor image quality should mainly meet the criteria：severe motion artifacts appeared in enhanced MRI images and thus cannot be used for further evaluation. Finally, among 66 volunteers, four were excluded due to undesirable image quality, eight were excluded due to atherosclerosis, 54 volunteers were in the final cohort.

MRI protocol

Prior to MR scanning, subjects were requested to fast at least 4 hours. MR images of the pancreases were acquired on a whole body 3.0 T MR scanner (Discovery MR750, GE Medical Systems, Chicago, IL, USA) with an eight-channel phased-array Torso coil. Using variable flip angle T1 mapping, pre-contrast three-dimensional spoiled gradient recalled echo sequence series were performed with flip angles of 3°, 6°, 9° and 12°. The other imaging parameters of T1 mapping were set as follows: repetition time (TR) = 3.2 msec, echo time (TE) = 1.5 msec, slice thickness = 4 mm, matrix = 260 x 160, field of view (FOV) = 360 x 360 mm^2. Then, DCE-MRI scans were performed by a three-dimensional fast spoiled gradient recalled echo sequence for liver acquisition with volume acceleration (LAVA) with the following parameters: TR = 3.2 msec, TE = 1.5 msec, flip angle = 12°, FOV = 360 x 360 mm^2, matrix = 260 x 160, slice thickness = 4 mm, bandwidth = 83.33 Hz/pixel. It took 240 sec to complete the DCE-MRI scanning with 40 phases acquired and 6 sec for each phase. After three pre-contrast phases were obtained, 0.1 mmol/kg of Gd-DTPA (Omniscan, GE Healthcare Co., Ltd., Shanghai, China) was administrated with a venous cannula at a rate of 2 ml/sec followed by a 20-ml saline flush at the same rate.

Data Manipulation

The DCE-MRI images were post-processed by Markov random fields (MRF) 3D non-rigid registration algorithms to correct motion artifacts. Then the images were transmitted to a workstation for quantitative analysis using DCE-MRI OK software package (Omni Kinetics, Version 2.00, GE Healthcare Co., Ltd.). The analysis process has the following steps. Firstly, the individual AIF was obtained from a region of interest (ROI) in abdominal aorta. Secondly, ROIs were manually drawn on pancreatic enhanced images on multiple slices without reaching the perimeter to avoid partial volume effect, meanwhile without inclusion of vessel and main pancreatic duct. Finally, ETL model[9, 10] was used to calculate the quantitative parameters: K^{trans}, k_{ep}, v_e and v_p. The mean of each parameter in the ROIs was used for statistical analysis.

The first observer (XXX) measured DCE-MRI pharmacokinetic parameters thrice (by a time interval of at least one week to eliminate memory effect) to evaluate intra-observer reproducibility. Then, each of the three observers (observer 1, XXX, observer 2, YYY, and observer 3, ZZZ) measured parameters once to examine inter-observer reproducibility.

Grouping

All subjects were divided into three groups owing to pancreatic region: pancreatic head (n = 54), body (n = 54) and tail (n = 54). Then, they were divided into three groups according to age: young (18 < age ≤ 40, median age 31, n = 18), middle (40 < age ≤ 60, median age 52, n = 18) and old-aged (age > 60, median age 68, n = 18), and two groups according to gender: male (n = 29) and female (n = 25).

Statistical Analyses

Intra- and inter-observer differences in pharmacokinetic parameters

Intra- and inter-observer differences were evaluated using one-way analysis of variance (ANOVA). Intra- and inter-observer agreements of pharmacokinetic parameters were evaluated using the inter-class correlation coefficient (ICC). The agreement was defined as good (ICC > 0.75), moderate (ICC = 0.5 - 0.75), or poor (ICC < 0.5). Coefficients of variation (CoV) were computed as the proportion of the standard deviation of the mean (standard deviation/mean, expressed as percentage). For CoVs concerning the intra-observer variability, standard deviation was computed over three measurements by one observer. For CoVs describing the inter-observer variability, standard deviation was computed over each parameter obtained by all three observers.

Differences of pharmacokinetic parameters among different region, age and gender groups

Shapiro Wilk test was used for the normality distribution test. If the data conformed to the normal distribution, One-way ANOVA test and Independent Two-sample t test were used to evaluate the differences of pancreatic pharmacokinetic parameters obtained by observer 1. The former test was performed to evaluate the differences of pancreatic pharmacokinetic parameters among different pancreatic regions and different age groups. And the latter was used to exam the differences of parameters between male and female groups.

All statistical analyses were performed with the SPSS software Version 19.0. *P* values < 0.05 were considered to indicate a statistically significant difference.

Results

Graphs of AIF, time-intensity curve (TIC) and images of quantitative parameters were achieved in all 54 subjects. A series of representative graphs of a volunteer were shown in Figure 1.

Intra- and inter-observer assessment for pharmacokinetic parameters

There were no statistically significant intra- or inter-observer differences for K^{trans}, k_{ep}, v_e and v_p (Table 1, *P* all > 0.10).

Agreement analysis: The intra- and inter-observer ICCs of K^{trans}, k_{ep}, v_e, v_p were 0.971, 0.952, 0.959, 0.944 and 0.947, 0.911, 0.978, 0.917, respectively. They were all greater than 0.90, which indicated excellent agreements (all $P < 0.001$) (Table 2).

Variability analysis: In both intra- and inter-observer analysis, the CoVs of K^{trans}, k_{ep}, v_e, v_p were 9.98%, 5.99%, 6.47%, 4.76% and 10.15%, 5.22%, 6.28%, 5.40%, respectively. They showed small variation (all CoVs < 10%), except for CoV of K^{trans} in inter-observer analysis (but only 10.15%) (Figure 2).

Differences of pharmacokinetic parameters among different region, age and gender groups

There were no significant differences of K^{trans}, k_{ep} and v_e among different pancreatic regions, the *P* values were all larger than 0.10. However, v_p of pancreatic head was significantly higher than that of pancreatic body and tail ($P = 0.014, 0.043$) (Table 3).

There were no significant differences to K^{trans}, k_{ep} and v_p among different age groups, the *P* values were all larger than 0.10. However, pancreatic v_e of old group was higher than that of young and middle-aged groups ($P = 0.042, 0.001$) (Table 4).

There were no significant differences to K^{trans}, k_{ep}, v_e and v_p between male and female groups, the *P* values were all larger than 0.10 (Table 5).

Discussion

In our evaluation of pancreatic DCE-MRI pharmacokinetic parameters, we used ETL model, which is a representative of two-compartment model. The model is generally recommended for tissue and tumor characterization, and computationally faster and better repeatability than the nonlinear method[17, 18]. Besides, Jesper et al has showed that linear model was more stable against time resolution reduction than nonlinear model [19]. In this study, we got pancreatic K^{trans}, k_{ep}, v_e and v_p values using ETL model. We found these pharmacokinetic parameters had an excellent reproducibility in intra- and inter-observer analysis. We also found pancreatic K^{trans} and k_{ep} were independent of pancreatic region, age and gender in healthy volunteers. However, v_p varied with pancreatic region and v_e varied with age. Our results

could provide a basis for further study on perfusion and permeability of diseased pancreas and selection of normal pancreas control. The choice of the normal control group is relative broadness in K^{trans} and k_{ep} assessment without considering the factors of pancreatic region, age and gender. However, for v_e and v_p, the choice of the normal control group should be prudent, because we found v_p varied with pancreatic region and v_e varied with age.

In our study, ICCs of K^{trans}, k_{ep}, v_e and v_p are all greater than 0.90, CoVs of these pharmacokinetic parameters are all less than 10% in intra- and inter-observer analysis except for K^{trans} (but only 10.15%) in inter-observer analysis. Our results are consistent with previous studies [20, 21] in DCE-MRI assessment of tumors. However, compared to their results, the parameters that we evaluated were more comprehensively. Our ICCs of v_p were higher and our CoVs of v_p were lower in intra- and inter-observer analysis than Wang et al [21]. This may be explained by a great deal of efforts made by us to ensure the precision of DCE-MRI. Before scanning, we made a strict implementation of inclusion and exclusion criteria, gave our technologists MRI scan training, and gave patients respiratory training. During scans, we used a series of 3D LAVA sequences, which can markedly reduce the scanning time compared with 2D sequences, but still maintain a high signal-to-noise ratio. After scanning, we used a 3D non-rigid image registration method to correct motion artifacts as much as possible. On the other hand, we chose to draw identical ROI on the abdominal aorta to obtain AIF, which was easy to operate and thus was more stable. In addition, we chose the ETL model, which might be more suitable to give more reliable and stable results [19]. Our results are different and superior to those of other researchers [22, 23], which is because they used different software to calculate DCE-MRI parameters and evaluate reproducibility. So, we should use single software to ensure very good reproducibility in a sequential study.

In our study, pancreatic v_p value was found varying among different region groups, which might be caused by the difference of their blood supply sources and blood vessels of the pancreatic islets in different regions. The arterial supplies of pancreas are complex, especially in pancreatic head[13]. The ratio of the capillary surface area to the volume of the islet capillaries was different between pancreatic head and caudal portion[24]. These might be the reason why v_p for pancreatic head is the highest among 3 groups. Bali MA et al [25] assessed pancreatic perfusion using DCE-MRI with and without secretin stimulation in healthy volunteers. In that study, they found distribution fraction were significantly different between the head and the body, tail without secretin stimulation. Distribution fraction is the volume fraction of the tissue that is accessible to the contrast agent, which corresponds to the plasma and the interstitial space. Our result showed that v_p for pancreatic head is the highest among 3 groups, which validates and deepens the above study, and indicated that the changing of distribution fraction may mainly come from the plasma space difference.

In our study, pancreatic v_e in old group was the highest among different age groups. Several reports demonstrated that there were significant correlations between pancreatic volume, parenchymal volume, fat volume, fat/parenchyma ratio, CT density and age[14, 26–28]. For instance, Caglar et al[14] found that pancreatic volume reached its maximum at the age of forty, and remained constant until age sixty, then decreased gradually. They also found that the CT density of the pancreas peaked at 50 years of age. Yang et al [26] found pancreatic fat fraction remained constant during the age of 20 to 40 years, but significantly increased during the ages of 41 to 50 and 51 to 70 years. Therefore, it is suspected that the v_e value is relative to pancreatic atrophy and fat replacement since their levels increase as the age grows.

Our study has some limitations. Firstly, ethical restrictions prevent repeated injection of contrast agents to volunteers, so there is a lack of assessment of san-rescan reproducibility. Secondly, due to the influence of the position of pancreas, respiration and the movement of surrounding organs, there are still slight artifacts and noises after registration. This is a technical problem that is difficult to avoid, but with the development of software and hardware, this condition would be improved.

In conclusion, DCE-MRI with ETL model can be applied to give a reliable, robust and reproducible quantitative assessment of pancreatic pharmacokinetic parameters noninvasively. K^{trans} and k_{ep} of pancreas are independent of pancreatic region, age and gender, but v_p can vary with pancreatic region and v_e can vary with age. Our study enriched the study of pharmacokinetics of normal pancreas and can also provide guidance for the selection of normal reference in the pharmacokinetics study of pancreatic diseases.

Declarations

Acknowledgements

The authors of this manuscript declare no any conflict of interest with any companies. No complex statistical methods were necessary for this paper. Thanks for Dr. Shi Zhongqiang, Dr. Zhu Feipeng and Professor Yang Weidong for the efforts of the fluency and readability of the manuscript.

Author contributions

Yong Yang, Zhiyong Quan and Weiwei Zhao designed the research. Yong Yang, Zhiyong Quan, Jing Yu and Yuyu Bi advanced the progress of the research and supervised the research group. Weiwei Zhao, Jing Yu, Yuyu Bi, and Zhiyong Quan collected, analyzed, interpreted the patient data and were major contributors in writing the manuscript. Yi Huan and Yong Yang assisted in interpreting the results. Yuanqiang Zhu, Jianmin Zheng and Weiqi Zhang performed the appointments and scanning of the subjects and provided technical support regarding the image post-processing.

Competing interests

The authors declare no competing interests.

References

1. Runge, V. M. et al. Intravascular contrast agents suitable for magnetic resonance imaging. *Radiology* 153, 171-176(1984).
2. Choyke, P. L. et al. Dynamic Gd-DTPA-enhanced MR imaging of the kidney: experimental results. *Radiology* 170, 713-720(1989).
3. El Sanharawi, I. et al. Non-palpable incidentally found testicular tumors: differentiation between benign, malignant, and burned-out tumors using dynamic contrast-enhanced MRI. *Eur J Radiol* 85, 2072-2082(2016).
4. Quarles, C. C., Bell L. C. & Stokes A. M. Imaging vascular and hemodynamic features of the brain using dynamic susceptibility contrast and dynamic contrast enhanced MRI. *Neuroimage* 187, 32-55(2019).
5. Zhang, M., Zhou, L., Huang, N., Zeng, H., Liu, S. & Liu, L. Assessment of active and inactive sacroiliitis in patients with ankylosing spondylitis using quantitative dynamic contrast-enhanced MRI. *J Magn Reson Imaging* 46, 71-78(2017).
6. Wáng, Y. X. J. et al. Topics on quantitative liver magnetic resonance imaging. *Quant Imaging Med Surg* 9, 1840-1890(2019).
7. Huang, W. et al. The Impact of Arterial Input Function Determination Variations on Prostate Dynamic Contrast-Enhanced Magnetic Resonance Imaging Pharmacokinetic Modeling: A Multicenter Data Analysis Challenge, Part II. *Tomography* 5, 99-109(2019).
8. van der Leij, C., Lavini, C., van de Sande, M. G. H., de Hair, M. J. H., Wijffels, C. & Maas, M. Reproducibility of DCE-MRI time-intensity curve-shape analysis in patients with knee arthritis: a comparison with qualitative and pharmacokinetic analyses. *J Magn Reson Imaging* 42, 1497-1506(2015).
9. Inglese, M. et al. Reliability of dynamic contrast-enhanced magnetic resonance imaging data in primary brain tumours: a comparison of Tofts and shutter speed models. *Neuroradiology* 61, 1375-1386(2019).
10. Zhai, J., Zheng, W., Zhang, Q., Wu, J. & Zhang, X. Pharmacokinetic analysis for the differentiation of pituitary microadenoma subtypes through dynamic contrast-enhanced magnetic resonance imaging. *Oncol Lett* 17, 4237-4244(2019).
11. Nagtegaal, I. D. et al. The 2019 WHO classification of tumours of the digestive system. *Histopathology* 76, 182-188(2020).
12. Guo, X. Y. et al. Exosomes and pancreatic diseases: status, challenges, and hopes. *Int J Biol Sci* 15, 1846-1860(2019).
13. Okahara, M., Mori, H., Kiyosue, H., Yamada, Y., Sagara Y. & Matsumoto S. Arterial supply to the pancreas, variations and cross-sectional anatomy. *Abdom Imaging* 35, 134-142(2010).
14. Caglar, V., Songur, A., Yagmurca, M., Acar, M., Toktas, M., & Gonul, Y. Age-related volumetric changes in pancreas: a stereological study on computed tomography. *Surg Radiol Anat* 34, 935-941(2012).
15. Klaassen, R. et al. Repeatability and correlations of dynamic contrast enhanced and T2* MRI in patients with advanced pancreatic ductal adenocarcinoma. *Magn Reson Imaging* 50, 1-9(2018).
16. Bali, M. A. et al. Tumoral and nontumoral pancreas: correlation between quantitative dynamic contrast-enhanced MR Imaging and histopathologic parameters. *Radiology* 261, 456-466(2011).
17. Filice, S. & Crisi, G. Dynamic contrast-enhanced perfusion MRI of high grade brain gliomas obtained with arterial or venous waveform input function. *J Neuroimaging* 26, 124-129(2016).
18. Jones, K. M., Pagel, M. D. & Cárdenas-Rodríguez, J. Linearization improves the repeatability of quantitative Dynamic Contrast-Enhanced MRI. *Magn Reson Imaging* 47, 16-24(2018).
19. Kallehauge, J. F., Sourbron, S., Irving, B., Tanderup, K. Schnabel, J. A. & Chappell, M. A. Comparison of linear and nonlinear implementation of the compartmental tissue uptake model for dynamic contrast-enhanced MRI. *Magn Reson Med* 77, 2414-2423(2017).
20. van den Boogaart, V. E. M. et al. Inter-reader reproducibility of dynamic contrast-enhanced magnetic resonance imaging in patients with non-small cell lung cancer treated with bevacizumab and erlotinib. *Lung Cancer* 2016, 93:20-27.

21. Wang, H. et al. Reproducibility of dynamic contrast-enhanced MRI in renal cell carcinoma: a prospective analysis on intra- and inter-observer and scan-rescan performance of pharmacokinetic parameters. *Medicine (Baltimore)* 94, e1529(2015).
22. Beuzit, L. et al. Dynamic contrast-enhanced MRI: study of inter-software accuracy and reproducibility using simulated and clinical data. *J Magn Reson Imaging* 43, 1288-1300(2016).
23. Marco Conte1, G. et al. Reproducibility of dynamic contrast-enhanced MRI and dynamic susceptibility contrast MRI in the study of brain gliomas: a comparison of data obtained using different commercial software. *Radiol Med* 122, 294-302(2017).
24. Vdovin, V. F. Blood vessels of the pancreatic islets in different portions of the adult human pancreas. *Arkh Anat Gistol Embriol* 76(2):44-48(1979).
25. Bali, M. A., Metens, T., Denolin, V., Maertelaer, V. D., Devière, J. & Matos, C. Pancreatic perfusion: noninvasive quantitative assessment with dynamic contrast-enhanced MR imaging without and with secretin stimulation in healthy volunteers-initial results. *Radiology* 247, 115-121(2008).
26. Yang, W., Xie, Y., Song, B., Xia, C., Tang, C. & Li, J. Effects of aging and menopause on pancreatic fat fraction in healthy women population. *Medicine (Baltimore)* 98, e14451(2019).
27. Chantarojanasiri, T., Hirooka, Y., Ratanachu-Ek, T., Kawashima, H., Ohno, E. & Goto, H. Evolution of pancreas in aging: degenerative variation or early changes of disease? *J Med Ultrason* 42, 177-183(2015).
28. Saisho, Y. et al. Pancreas volumes in humans from birth to age one hundred taking into account sex, obesity, and presence of type-2 diabetes. *Clin Anat* 20, 933-942(2007).

Tables

Table 1 Pancreatic Pharmacokinetic Parameters of DCE-MRI and Intra-, Inter-observer Difference Analysis

	Intra-observer				Inter-observer			
	1st Measure-ment	2nd Measure-ment	3rd Measure-ment	*P*	Observer 1	Observer 2	Observer 3	*P*
K^{trans}	0.0621±0.0059	0.0610±0.0061	0.0618±0.0064	0.627	0.0621±0.0059	0.0610±0.0063	0.0611±0.0065	0.614
k_{ep}	0.1065±0.0071	0.1073±0.0066	0.1067±0.0055	0.834	0.1065±0.0071	0.1069±0.0044	0.1063±0.0049	0.861
v_e	0.6098±0.0408	0.6031±0.0417	0.6116±0.0353	0.494	0.6098±0.0408	0.6027±0.0346	0.6063±0.0389	0.627
v_p	0.2479±0.0126	0.2452±0.0124	0.2458±0.0102	0.467	0.2479±0.0126	0.2434±0.0131	0.2467±0.0140	0.194

Table 2 Agreement Analysis on Pancreatic Pharmacokinetic Parameters of DCE-MRI

-	Intra-observer		Inter-observer	
	ICC (95% CI)	*P*	ICC (95% CI)	*P*
K^{trans}	0.971(0.955, 0.982)	< 0.001	0.947(0.917, 0.968)	< 0.001
k_{ep}	0.952(0.924, 0.970)	< 0.001	0.911(0.860, 0.946)	< 0.001
v_e	0.959(0.936, 0.975)	< 0.001	0.978(0.965, 0.986)	< 0.001
v_p	0.944(0.913, 0.966)	< 0.001	0.917(0.870, 0.949)	< 0.001

Table 3 Comparison of Pancreatic Pharmacokinetic Parameters among Different Pancreatic Regions

	N	K^{trans} (ml/min)	k_{ep} (ml/min)	v_e (ml/ml)	v_p (ml/ml)
Head	54	0.0621±0.0044	0.1068±0.0052	0.6156±0.0395	0.2509±0.0042[a, b]
Body	54	0.0615±0.0042	0.1068±0.0054	0.6041±0.0382	0.2456±0.0029[a]
Tail	54	0.0622±0.0044	0.1061±0.0043	0.6063±0.0354	0.2460±0.0043[b]
F		0.428	0.367	1.423	3.521
P		0.653	0.694	0.244	0.032

Note: **[a, b]** indicate there was statistically difference between the two corresponding groups. [a] shows $P = 0.014$, [b] shows $P = 0.043$. Head, pancreatic head group, Body, pancreatic body group, Tail, pancreatic tail group

Table 4 Comparison of Pancreatic Pharmacokinetic Parameters among Different Age Groups

	N	K^{trans} (ml/min)	k_{ep} (ml/min)	v_e (ml/ml)	v_p (ml/ml)
Youth	18	0.0621±0.0044	0.1063±0.0048	0.6082±0.0405[a]	0.2472±0.0066
Middle	18	0.0615±0.0042	0.1064±0.0053	0.5994±0.0344[b]	0.2477±0.0063
Old	18	0.0622±0.0044	0.1071±0.0050	0.6225±0.0333[a, b]	0.2476±0.0074
F		0.428	0.416	5.591	0.090
P		0.653	0.660	0.005	0.914

Note: **[a, b]** indicate there was statistically difference between the two corresponding groups. [a] shows $P = 0.042$, [b] shows $P = 0.001$. Young, young age group, Middle, middle age group, Old, old age group

Table 5 Comparison of Pancreatic Pharmacokinetic Parameters between Different Gender Groups

	N	K^{trans} (ml/min)	k_{ep} (ml/min)	v_e (ml/ml)	v_p (ml/ml)
Male	29	0.0615±0.0045	0.1065±0.0049	0.6055±0.0379	0.2473±0.0067
Female	25	0.0625±0.0040	0.1066±0.0051	0.6124±0.0377	0.2478±0.0068
t		-1.415	-0.139	-1.160	-0.492
P		0.159	0.889	0.248	0.623

Male, male group, Female, female group

Figures

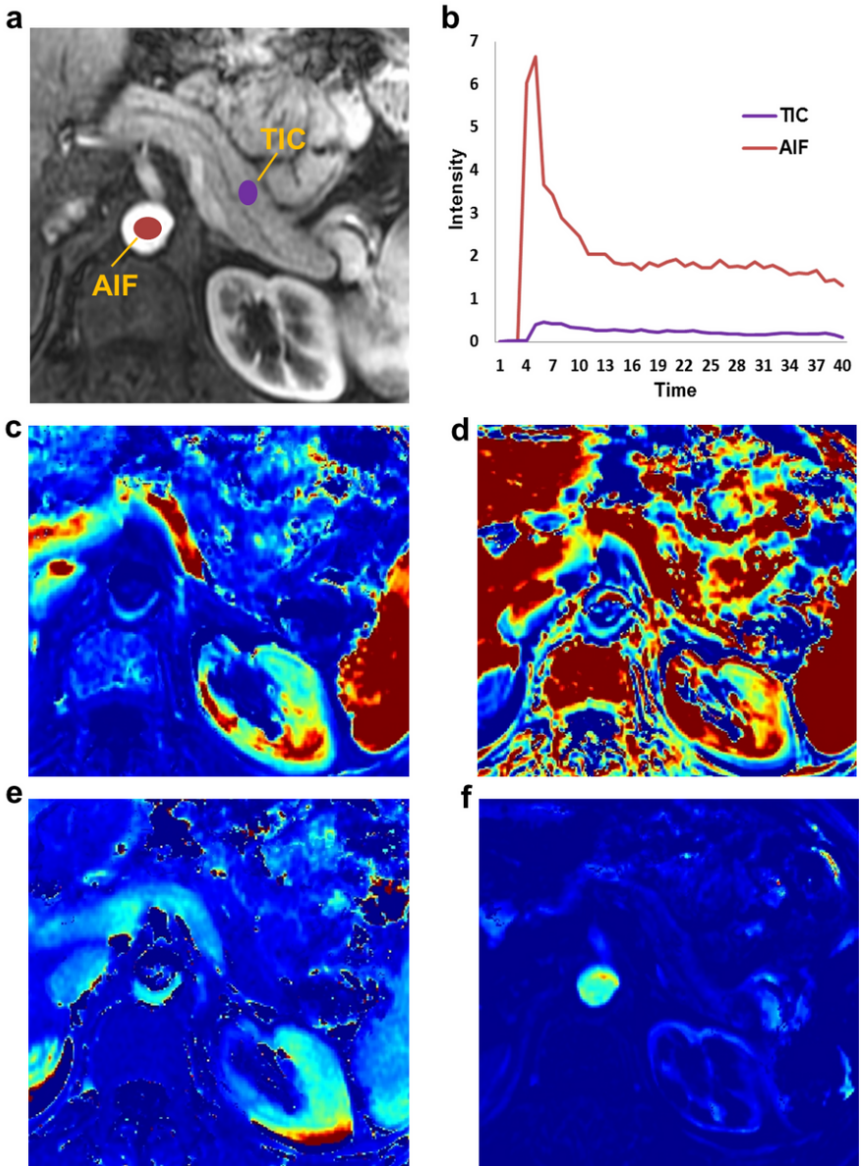

Figure 1

Images of a subject show the process of DCE-MRI quantitative analysis. a is enhanced image shows the drawing of ROIs when calculating AIF and TIC, b shows graphs of AIF and TIC of relevant ROIs of image a, c is Ktrans image, d is kep image, e is ve image, and f is vp image. DCE-MRI, dynamic contrast-enhanced magnetic resonance imaging, ROI, region of interest, AIF, arterial input function, TIC, time-intensity curve, Ktrans, volume transfer constant, kep, contrast transfer rate constant, ve, extravascular extracellular space volume fraction, vp, plasma volume fraction

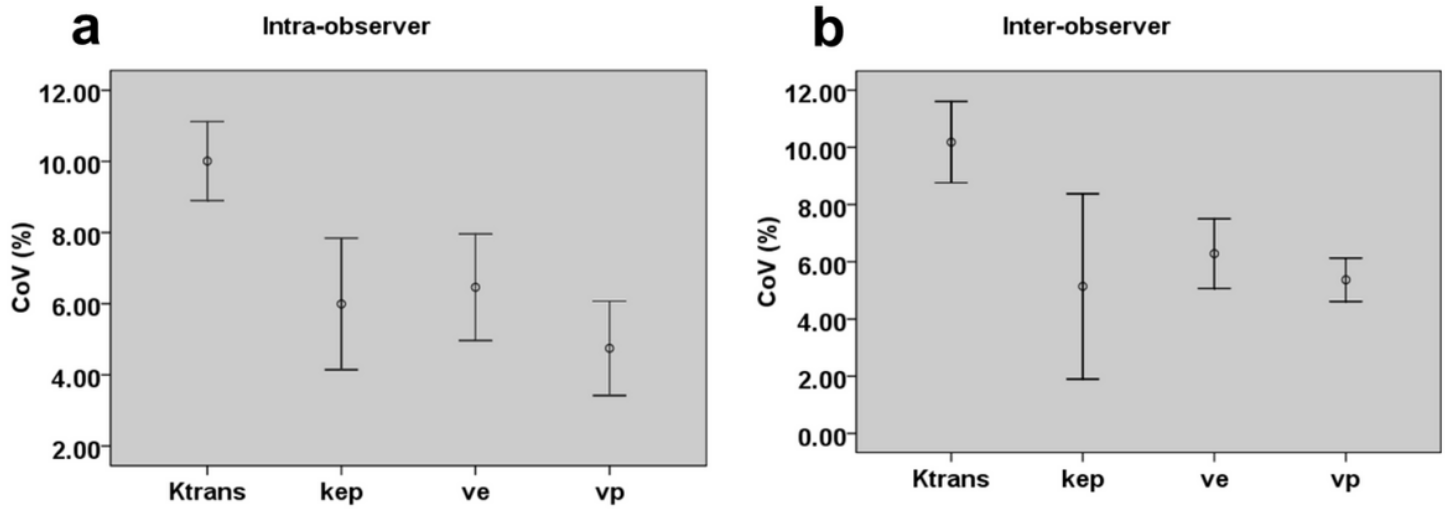

Figure 2

Variability analysis of intra-observer and inter-observer. The intra-observer (a) and inter-observer (b) CoV (%) values of Ktrans, kep, ve and vp. All data are presented as mean and 95% confidence interval. CoV, coefficient of variation, Ktrans, volume transfer constant, kep, contrast transfer rate constant, ve, extravascular extracellular space volume fraction, vp, plasma volume fraction